

Effect of Heat Treatments on the Mechanical and Microstructure Properties of Welded API X70 Steel



Aboubaker Haissam^{1*}, Souad Benarrache^{1,2}, Rabeh Kouider Rahmani³, Tahar Mansouri⁴,
Mohammed Elhadi Benhorma¹

¹ Mechanical Laboratory, Amar Telidji University of Laghouat, Laghouat 03000, Algeria

² ENS Laboratory, Ecole Normal Supérieure de Laghouat, Laghouat 03000, Algeria

³ Modelling, Simulation and Optimization of Real Complex Systems Research Laboratory, Ziane Achour University of Djelfa, Djelfa 17000, Algeria

⁴ Laboratory Process Engineering, University of Laghouat, Laghouat 03000, Algeria

Corresponding Author Email: haissambakar@gmail.com

Copyright: ©2024 The authors. This article is published by IETA and is licensed under the CC BY 4.0 license (<http://creativecommons.org/licenses/by/4.0/>).

<https://doi.org/10.18280/acsm.480412>

ABSTRACT

Received: 5 March 2024

Revised: 19 July 2024

Accepted: 1 August 2024

Available online: 30 August 2024

Keywords:

X70 API, weld joints, heat treatments, fusion zone (FZ), X-ray diffraction, grain growth, hardness, scanning electron microscope (SEM)

The world race in scientific research in the fields of petroleum and how petroleum is transported to another place has inspired our scientific curiosity to research the welding bead of petroleum pipelines. This paper is an experimental examination of the response to the effect of heat treatments on the mechanical and microstructure properties of welded API X70 steel. Our study investigates how heat treatments altered the microstructure and mechanical properties of the fusion zone (FZ) in welded pipe steel of grade API X70. It shows microstructures achieved after one heat treatment at 550°C for 1h, 2h, 3h, 4h and 5h. A metallographic test by the optical microscope and the scanning electron microscope (SEM) as well as the analysis of the samples by X-ray diffraction (XRD) and the measurement of the hardness test was applied to all the samples prepared. The results revealed that the isothermal heat treatment caused grain growth and coarsening reactions in the weld zone and the hardness of weld joints decreased were the main transformations after increasing the temperature of the heat treatment.

1. INTRODUCTION

The world of industry in the domain of hydrocarbons and transport has undergone important developments thanks to the mastery of the mechanical and structural properties of HSLA steels. The temperature and holding time have an important effect on the development of the structural characteristics of the steel (X70 API); which afterwards directly affects the mechanical properties, notably the resistance to rupture under the effect of high stresses.

In the realm of metallurgy, where the properties of metals are carefully manipulated, one key player is carbon. The carbon atoms can fit into the free spaces between the atoms of the FCC iron. Solubility varies with temperature. The solid solution of carbon in (γ iron) is called austenite. The one formed in (iron α) is called ferrite. Remember that carbon is very poorly soluble in α -iron. Due to variations in solubility of carbon, the latter is dissolved in iron γ , then it is rejected in the form of precipitates of Fe_3C , or cementite during cooling. The Fe_3C alloy is hardened by these carbides. This precipitation depends on temperature and time. The equilibrium diagram presents two domains, (iron α + iron γ) and (iron γ + cementite) which have in common a point corresponding to 727°C and 0.77% C (by weight); such an alloy undergoes a eutectoid transformation at 727°C [1, 2].

The welding of API X70 steels holds crucial significance in

the pipeline industry, where these materials are extensively employed for the transportation of high-pressure fluids in the oil and gas sector. API X70 steel is renowned for its high mechanical properties, corrosion resistance, and ability to withstand severe operating conditions. However, the welding process of these steels poses particular challenges due to their complex chemical composition and specific performance requirements. Welding API X70 steel involves the successive melting and solidification of the material, creating thermally affected zones and fundamental zones in the welded region. These zones undergo microstructural transformations and changes in mechanical properties that can influence the reliability and durability of the welded material. Understanding these transformations is essential to ensure the structural integrity of pipelines under diverse operating conditions. Welding is a process which is characterized by a great complexity of physico-chemical phenomena and the parameters which come into play. In welding, the atomic bond produced at the joint requires the intervention of an external energy source which creates a rise in temperature in the rooms. The energy sources used are electrical, chemical, mechanical (friction) or optical (Laser). Steel is the easiest metal to weld because it can be used to produce the full range of welding processes [3].

Heat treatment can induce significant microstructural transformations in the weld zone, affecting essential

mechanical properties such as strength, hardness, ductility, and toughness. A thorough understanding of these effects is therefore necessary to predict the long-term behavior of welds and to optimize welding parameters in order to minimize defects and potential weak spots. Previous studies have shown that microstructural transformations can strongly depend on the cooling conditions and thermal cycles imposed during the welding process [4, 5].

Existing literature has explored various aspects of welds on API steels, including the types of defects that may occur, detection methods, and techniques for improving welds. However, there is a crucial need for more detailed research on the microstructural evolution in the weld zone in response to heat treatments. Such a study would allow the development of more accurate predictive models for weld performance, leading to improved manufacturing and maintenance practices for pipelines. For example [6], demonstrated that post-weld heat treatments can significantly improve the resistance to cracking in weld zones.

Furthermore, the study of microstructural evolution is essential to understand the fundamental mechanisms that govern the formation and growth of metallurgical phases in the weld zone. This includes grain formation, secondary phase precipitation, and alloying element distribution. These microstructural aspects directly impact the mechanical properties of the weld and, consequently, the overall structural integrity of pipelines. Recent research has highlighted the importance of these factors for the durability of welds [7].

The refining of grains can be greatly affected by Niobium, just like aluminum, and the critical particle size is approximately 300 Angstroms, just like AlN. Lastly, the addition of Al and Nb together has a slightly higher efficiency than that of Al alone [8-11]. The formation of two compounds of titanium includes TiN, which is an exceptionally stable precipitate and nearly insoluble in austenite [12-14], and TiC carbide. Titanium not trapped by nitrogen forms a carbon-rich carbonitride of diameter about 200 Å, which dissolves in the austenite up to about 1300°C. The grain's growth is controlled by this carbide.

Chromium in small quantities improves mechanical characteristics and heat treatments such as hardenability. High chromium contents provide resistance to abrasion and oxidation. It can have a concentration of up to 1% in HSLA steels; It improves mechanical properties without compromising weldability and low temperature resistance, and increases the bainite fraction and breaking strength; It increases resistance to atmospheric corrosion and when present in combination with copper and/or phosphorus, it increases resistance to seawater corrosion [15, 16].

In this work we carried out a series of analyzes at different temperatures and holding times, with the aim of following the development of the microstructure and the mechanical property. The objective of our paper work is a structural characterization of the weld bead (fusion zone) of a high strength HSLA steel.

2. EXPERIMENTAL METHODS

The material used in our study is the weld bead of X70 steel whose length is 400 mm and its thickness is 15 mm. The material used and deposited metal whose chemical composition is given in the following Figure 1 and Figure 2. This is classified under API standard 5L5L (American Petroleum Institute Specification for Pipeline) [17].

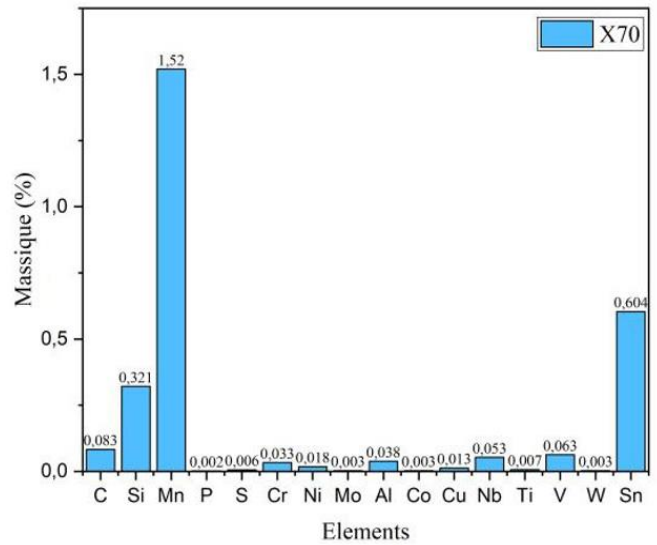


Figure 1. Chemical composition of X70

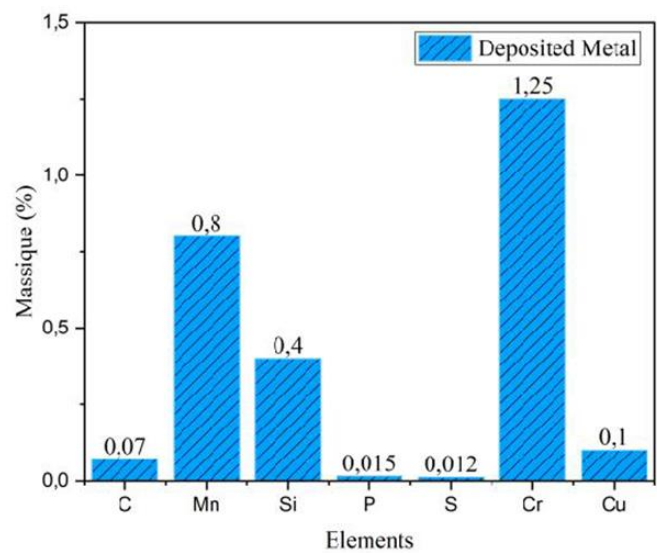


Figure 2. Chemical composition of deposited metal

The heat treatments conducted in this study were performed using a NABERTHERM electric furnace. This furnace features an insulated chamber measuring 700 × 500 × 250 mm, with temperature regulation provided by a resistance heater, capable of reaching a maximum heating capacity of 3000°C. At the bottom of the chamber, the sample maintains a completely homogeneous temperature, with a temperature gradient of less than 5°C between different points on the sample. In our study, we will apply one heat treatment protocols: consists in setting the temperature of the heat treatment at 550°C and we vary the holding time (1h, 2h, 3h, 4h, 5h) as illustrated in Figure 3. After heating, the samples underwent air cooling at room temperature 25°C.

To reveal the microstructure of the samples after heat treatment, the samples are mechanically polished using silicon carbide abrasive papers of various grades: 80, 400, 600, 800, and 1200 μm. The preparation continues with final polishing using diamond paste with grain sizes of 0.25 μm, until a mirror-like surface is obtained. This procedure allowed us to achieve metallurgical mirror finishes. The samples are then etched with a Nital solution (composed of 4% nitric acid and 96% ethanol) for approximately 30 to 60 seconds to reveal the microstructure, which causes the mirror-like finish to

disappear. Following this, the samples are rinsed with water to halt the etching process. The samples are analyzed using two types of microscopes. First, an optical microscope (LIECA DMLM) equipped with a high-resolution camera is employed to observe the samples at a magnification of 1000x. Following this, a TESCAN VEGA3 scanning electron microscope (SEM), featuring a thermal emission tungsten source, is used for detailed examination. This SEM system is optimized for both high and low vacuum operations, providing enhanced imaging and analysis capabilities. Grain size was measured using the line-intercept method as described in ASTM E112- 13 by ImageJ software, Grain size on function of time is given by Table 1. SEM micrographs were taken at 20 μm magnification, and at least five fields of view were analyzed for each sample. The average grain diameter was calculated by counting the number of grain boundary intersections along a known length of test lines superimposed on the micrographs.

Table 1. Grain size (μm) on function of time

| | 1h | 2h | 3h | 4h | 5h |
|-------|------|------|-------|-------|-------|
| 550°C | 5.14 | 8.01 | 10.02 | 12.04 | 13.78 |

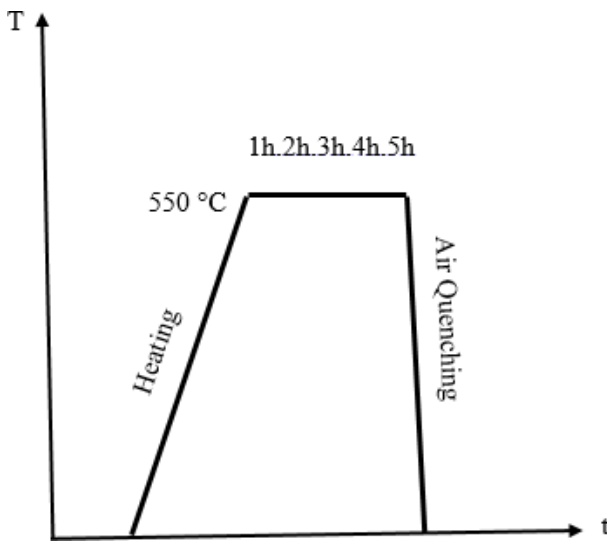


Figure 3. Heat treatment

In a Vickers hardness test, the indenter is a square-based diamond pyramid with a top angle of 136°. The resulting indentation is therefore pyramidal. The Vickers hardness HV is calculated using the following Eq. (1).

$$Hv = 1.8544 F / d^2 \quad (1)$$

where, F is the applied force and d is the average length of the diagonals of the indentation. A total of six Vickers hardness measurements were performed on the samples using a Model MVK-H2 durometer (Hardness Testing Machine) with a load of 300 g. These measurements were conducted on the same samples that were analyzed in the metallographic study.

The diffraction measurements were carried out by means of a beam X-ray diffractometer XRD Panalytical Empyrean. The X-ray are generated by a Cu anode $k\alpha=1,54060 \text{ \AA}$. The operating parameters for all the samples are 1 kV and 1 mA with a step of $0,0260^\circ$ and a fixation time of 116,7900 second for each step. The scanning is carried out over a range 2θ of $(20^\circ - 120^\circ)$ with rotation by time of 30 min.

3. RESULTS AND DISCUSSION

3.1 Effect of heat treatment on microstructures

Figure 4 presents a micrograph of the weld bead, two different zones of which we speak of the fusion zone and the base metal. The micrograph of base metal (Figure 4a) consisting an equiaxed ferritic and pearlitic matrix [18]. The micrograph of fusion zone (Figure 4b) consisting a ferritic acicular and pearlitic region. Figure 5 presents a micrograph of fusion zone at 550 with different time. The microstructure of the fusion zone (FZ) in welded API X70 steel exhibited distinct changes following different time. At 1h, the microstructure consists of an equiaxed ferritic and fine pearlitic matrix. The presence of these phases indicates the initial stability of the weld zone with fine grains, which is typical after short heat treatments (Figure 5).

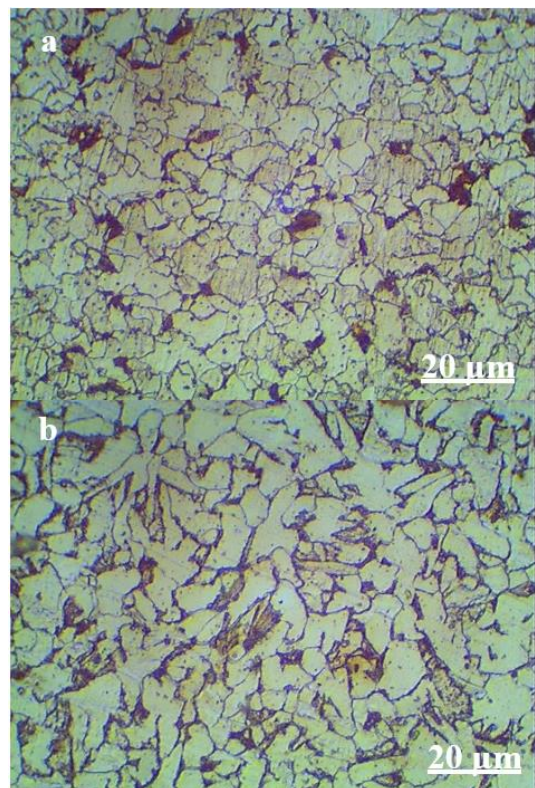
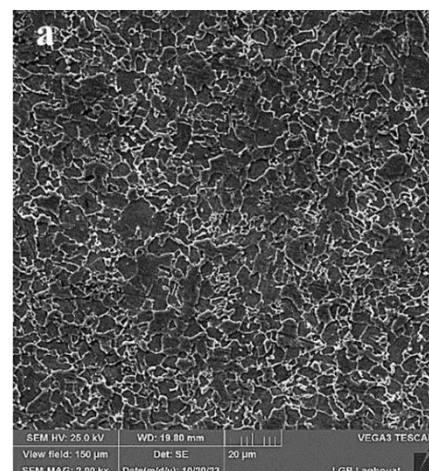


Figure 4. Optical micrograph of the weld bead of a) base metal b) fusion zone



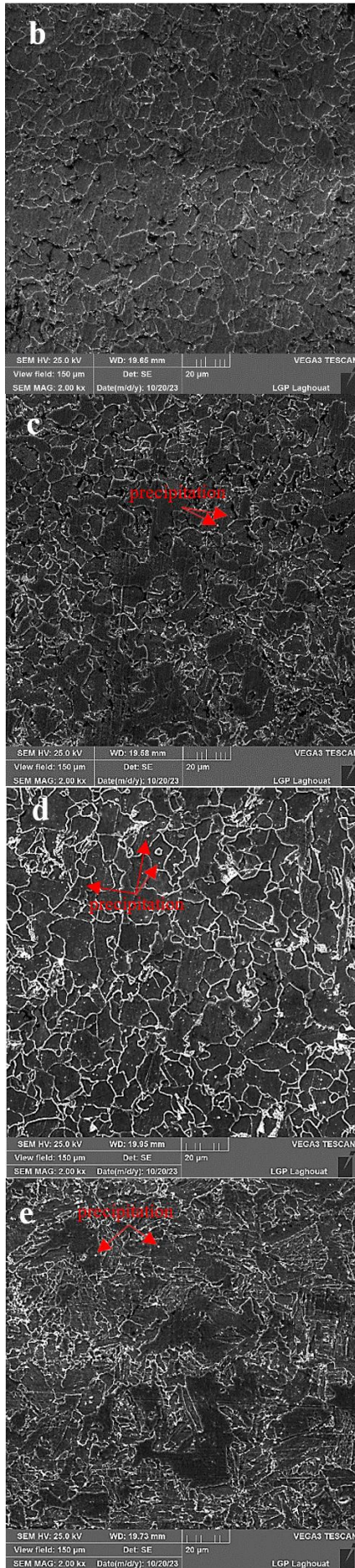


Figure 5. SEM micrograph of the fusion zone at 550 of a) 1h b) 2h c) 3h d) 4h e) 5h

At 2h, the grain growth becomes evident. The increase in grain size can be attributed to prolonged exposure to heat, which provides sufficient energy for grain boundary movement and coalescence of smaller grains into larger ones. This is consistent with the observations in previous studies on steel weldments subjected to heat treatment [19]. When the time increase at 3h the grains continue to grow, and Chromium carbide and Nickel carbide precipitates start to form (Figure 6c and Figure 6d). The formation of these carbides can be explained by the diffusion of alloying elements such as Chromium and Nickel, which form stable carbide phases at elevated temperatures. This increase is always explained by a gain in energy (heat input) which always directs the system (the matrix, addition elements and the different phases) towards a stable thermodynamic equilibrium. This which is strongly affected by the addition elements and the energies of point and linear defects (internal stresses) as well as the interfacial tensions between the grains; these which change depending on the size of the grains in this system we can illustrate thermodynamic equilibrium by the free enthalpy equation Eq. (2).

$$\Delta G = \Delta H - T\Delta S + \sum_i^n Q_i \quad (2)$$

At temperatures T the system is in equilibrium when

$$\frac{\partial G}{\partial T} = 0 \quad (3)$$

where, ΔG is the change in free energy, ΔH is the change in enthalpy, T is the temperature, ΔS is the change in entropy, and Q_i represents the energies of point and linear defects as well as interfacial tensions between grains and dislocations [20]. At 5h, further microstructural changes include the formation of Chromium carbide and bainite (Figure 6e). The formation of bainite, a phase known for its toughness and strength, indicates significant transformation in the microstructure due to the extended heat treatment time [21].

3.2 X-ray analysis

The x-ray diffraction diffractograms in Figure 6, show the samples from the FZ. While at 550°C and with a holding time of 5 hours, we note the diffraction angles 2θ : (44,5990°), (64,991°), (82,435°), (98,849°) and (116,49°) with a shift of the peaks relative to 1 hour of: (44,1429°), (64,410°), (82,248°), (98,777°), and (116,161°), this shift of the peaks and the variation of the intensities of the diffracted peaks, informs us about the quantity of the different densities of the diffracted planes during the formation and/or dissolution of the different phases, case of Chromium or Nickel.

X-ray diffraction analysis of steel X70 samples heat-treated at 550°C for holding times ranging from 1 to 5 hours revealed the presence of several coexisting phases: the iron matrix (Fe), iron carbide (Fe_3C), aluminum nitride (AlN), chromium iron (CrFe), nickel iron (FeNi), and chromium (Cr). The micrograph (Figure 5) depicts a progressive increase in grain size with increasing holding time. At the 2-hour, the diffractograms (Figure 6b) is dominated by the (200) reflection of AlN, indicating its predominant presence. However, the presence of Fe_3C is also evident through its (102) and (220) reflections. For holding times between 3 and 5 hours, the reappearance of CrFe, FeNi, and Cr phases becomes significant in the diffractograms (Figures 6c, 6d, and 6e), as

evidenced by the emergence of their respective (011), (111), and (211) reflections.

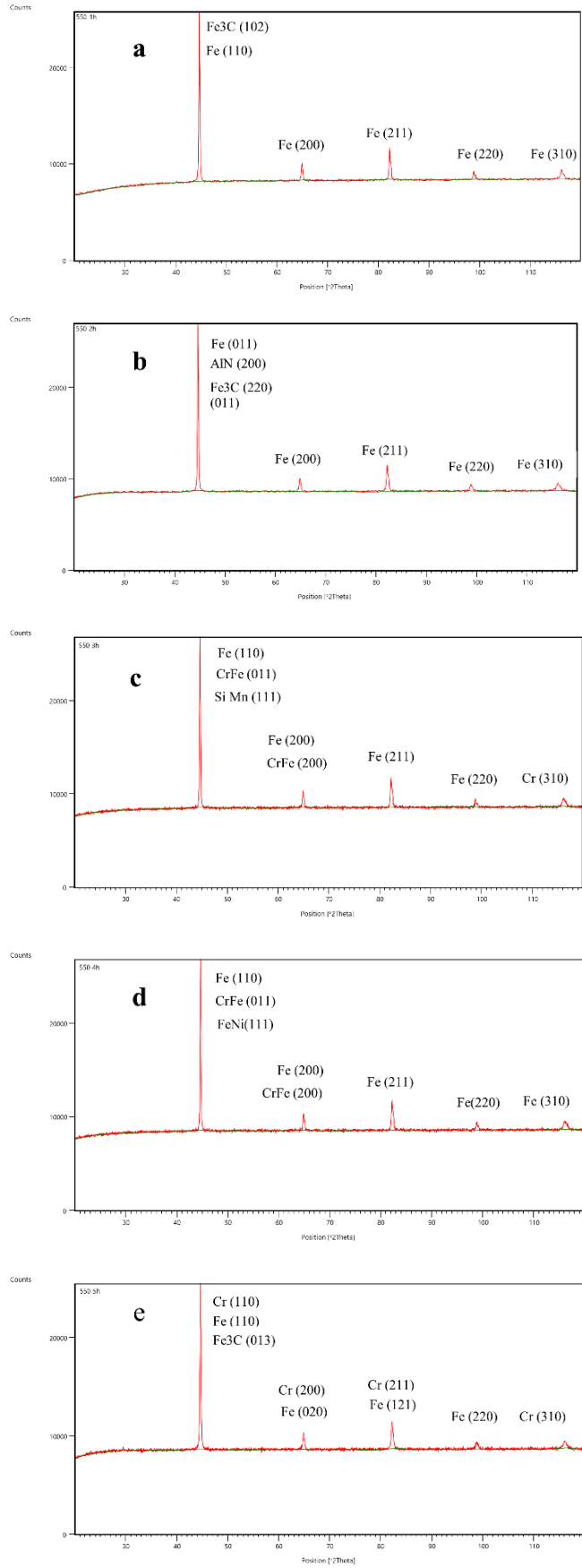


Figure 6. Diffractogram of the fusion zone (FZ) of the weld seam under 550°C heat treatment for a holding time of a) 1h b) 2h c) 3h d) 4h e) 5h

3.3 Effect of heat treatment on hardness

Figure 7 presents the HV hardness as a function of time. we notice that with increasing time the hardness decreases. 230 HV to 170 HV, due of carbide precipitation (Cr and Ni), grains size and the dissipation of dislocations (internal stresses) [22]. The formation of Chromium and Nickel carbides consumes the alloying elements, which leads to a decrease in solid solution strengthening. As these carbides precipitate out of the matrix, the matrix itself becomes softer, contributing to the overall reduction in hardness. Prolonged heat treatment leads to grain growth, which reduces the grain boundary area per unit volume. According to the Hall-Petch relationship [23, 24], an increase in grain size results in lower hardness and yield strength. The Hall-Petch relationship can be expressed as Eq. (3).

$$\sigma_y = \sigma_0 + k_y \cdot d^{-1/2} \quad (4)$$

σ_y is the yield stress, σ_0 is a material constant, k_y is the strengthening coefficient, d is the average grain diameter.

As the grains grow, the material's resistance to deformation decreases, thereby reducing the hardness. The reduction in hardness is also influenced by the dissipation of dislocations, which are key to strengthening the material. The mobility of dislocations can be described by the equation Eq. (4).

$$V = \alpha \exp((-\Delta Hi)/RT) \quad (5)$$

where,

V: dislocation mobility speed.

ΔHi : Enthalpy of activation of a dislocation at temperature T.

This speed of dissipation and measured in pure grains (Exp: Fe) in our case this speed will depend enormously on the impurities in the grains, namely the existence of different addition elements in the interstice or carbides by an area of the matrix.

Overall, the combined effects of carbide precipitation, grain growth, and dislocation dissipation lead to the observed decrease in hardness with increasing time.

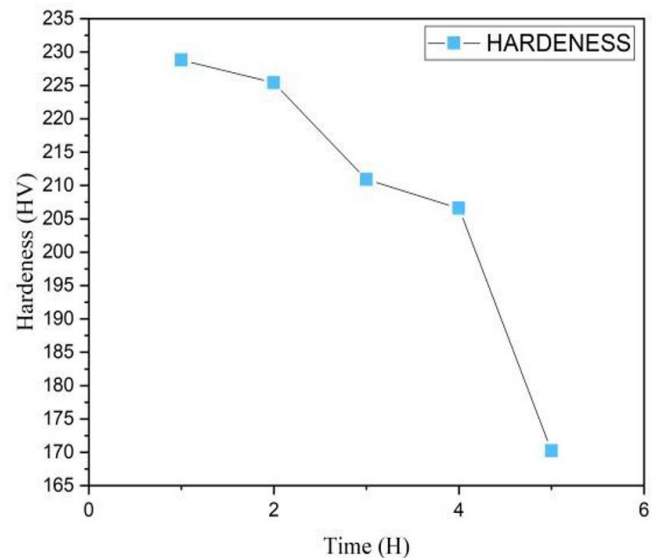


Figure 7. Hardness measurement at 550°C

4. CONCLUSIONS

The evaluation of heat treatments on the mechanical and microstructure properties of welded API X70 steel allowed us to put forward the following conclusions:

1. The study observed significant shifts in diffraction angles (2θ) from 44.1429° , 64.410° , 82.248° , 98.777° , and 116.161° at 1 hour to 44.5990° , 64.991° , 82.435° , 98.849° , and 116.49° at 5 hours. These shifts suggest variations in the density of diffracted planes, indicative of phase formation or dissolution processes involving elements such as Chromium and Nickel. This finding underscores the sensitivity of diffraction techniques in monitoring phase changes during heat treatment. This new insight into the phase dynamics during heat treatment provides a deeper understanding of the microstructural evolution in API X70 steel.
2. The increase in grain size and the formation of carbide precipitates (Cr and Ni) over time indicate that prolonged heat treatment leads to significant microstructural evolution. At 3 hours, the formation of carbide precipitates and increased grain size are notable, and by 5 hours, further grain growth and the appearance of chromium carbide precipitates are observed. These changes are critical in understanding the evolution of microstructure with extended heat treatment durations.
3. The decrease in hardness from 230 HV at 1 hour to 170 HV at 5 hours can be attributed to carbide precipitation, increased grain size, and the dissipation of internal stresses. This reduction in hardness highlights the trade-off between hardness and microstructural changes. This novel finding emphasizes the need for precise control of heat treatment parameters to balance mechanical properties and ensure optimal performance.

The findings have implications for the performance of API X70 steel in applications where heat treatment processes are used to achieve desired mechanical properties. Understanding the trade-offs between hardness, grain size, and phase composition can help in optimizing heat treatments for specific industrial applications, such as in pipelines or structural components. The insights into microstructural changes and their effects on hardness can be applied to other structural components made from API X70 steel, ensuring that heat treatment processes meet the required specifications for strength and durability.

The suggested research directions for Investigating the influence of other alloying elements on phase behavior and mechanical properties could provide a more comprehensive understanding of their effects on heat treatment outcomes. Conducting real-world performance tests, such as fatigue and impact tests, could validate the research findings and assess their applicability in practical scenarios.

REFERENCES

- [1] Callister, W.D. (2020). *Materials Science and Engineering: An Introduction*. John Wiley & Sons.
- [2] Dupeux, M. (2008). *Aide-Mémoire de Science des Matériaux - 2ème Édition*. Dunod.
- [3] Jeffus, L. (2021). *Welding: Principles and Applications (9th ed.)*. Cengage Learning.
- [4] Ming, Z., Wang, K.H., Liu, Z., Wang, W., Wang, Y.Q. (2020). Effect of the cooling rate on the microstructure

- and mechanical properties of high nitrogen stainless steel weld metals. *China Welding*, 29(2): 48-52. <https://doi.org/10.12073/j.cw.20200221002>
- [5] Shrahan, C., Radhika, N., NH, D.K., SivaSailam, B. (2023). A review on welding techniques: Properties, characterisations and engineering applications. *Advances in Materials and Processing Technologies*, 10: 80. <https://doi.org/10.1080/2374068X.2023.2186638>
 - [6] Chen, G., Xue, W., Jia, Y., Shen, S., Liu, G. (2020). Microstructure and mechanical property of WC-10Co/RM80 steel dissimilar resistance spot welding joint. *Materials Science and Engineering: A*, 776: 139008. <https://doi.org/10.1016/j.msea.2020.139008>
 - [7] Singh, M.P., Shukla, D.K., Kumar, R., Arora, K.S. (2021). The structural integrity of high-strength welded pipeline steels: A review. *International Journal of Structural Integrity*, 12(3): 470-496. <https://doi.org/10.1108/IJSI-05-2020-0051>
 - [8] Constant, A., Grumbach, M., Blood, G. (1970). Study of the transformation of the austenite and changes the properties of steels at dispersoids. *Metallurgy Review*.
 - [9] CSM. (1971). *Study of the Influence of Niobium*. ECSC Information Days Luxembourg.
 - [10] Gladman, T. (1966). On the theory of the effect of precipitate particles on grain growth in metals. *Proceedings of the Royal Society of London. Series A. Mathematical and Physical Sciences*, 294(1438): 298-309.
 - [11] Ling, Z.Q., Fang, J., Zhou, Y., Yuan, Z.X. (2012). Influence of quenching on-line on properties of X70 steel for sour service seamless pipe. *Energy Procedia*, 16, 444-450. <https://doi.org/10.1016/j.egypro.2012.01.072>
 - [12] Zhao, A.M., Wang, Y., Chen, Y.L., Tang, D., Gao, X.T., Zuo, B.Q. (2011). Precipitation behaviors of X80 acicular ferrite pipeline steel. *International Journal of Minerals, Metallurgy, and Materials*, 18: 309-313. <https://doi.org/10.1007/s12613-011-0439-4>
 - [13] Bridge, G., Maynier, P., Dollet, J., Bastien, P. (1970). Contribution to the study of the influence of molybdenum on the softening of activation energy income. *Metallurgical News*.
 - [14] Lewellym, D.T., Cook, W.T. (1974). Metallurgy of boron tread low-alloy steel. *Metals Technology*, 1(1): 517-529. <https://doi.org/10.1179/030716974803287924>
 - [15] Murry, G. (1980). Transformations dans les aciers. *Techniques de L'ingénieur*. <https://doi.org/10.51257/a-v1-m1115>
 - [16] Benarrache S., Benchatti T., Benhorma H.A. (2019). Formation and dissolution of carbides and nitrides in the weld seam of X70 steel by the effects of heat treatments. *Annales de Chimie: Science des Matériaux*, 43(1): 11-16. <https://doi.org/10.18280/acsm.430102>
 - [17] NORME API 1104_Fr_Ed.99. (1999). *Soudage de canalisations et installations connexes Segment canalisations*. Norme API 1104 Dixneuvieme Edition. Institut Américain du Pétrole. <https://pdfcoffee.com/api-1104fred99-pdf-free.html>.
 - [18] Lawal, S.L., Afolalu, S.A., Jen, T.C., Akinlabi, E.T. (2023). Effects of varying microstructural constituents on corrosion resistance: A review. *Revue des Composites et des Matériaux Avancés-Journal of Composite and Advanced Materials*, 33(2): 95-101. <https://doi.org/10.18280/rcma.330204>
 - [19] Kou, S. (2003). *Welding Metallurgy*. Wiley-Interscience.

- [20] Porter, D.A., Easterling, K.E. (1992). Phase Transformations in Metals and Alloys. CRC Press. <https://doi.org/10.1201/9781439883570>
- [21] Bhadeshia, H.K.D.H. (2001). Bainite in Steels: Transformation, Microstructure and Properties. London: IOM, pp. 237-276.
- [22] SAMI, Z., Omar, A. (2022). Effects of the tempering temperature on microstructure and mechanical properties of X70 dual phase steel. Metallurgical and Materials Engineering, 28(2): 351-358. <https://doi.org/10.30544/753>
- [23] Hall, E.O. (1951). The deformation and ageing of mild steel: III discussion of results. Proceedings of the Physical Society, Section B, 64(9): 747. <https://doi.org/10.1088/0370-1301/64/9/303>
- [24] Petch, N.J. (1953). The cleavage strength of polycrystals. Journal of the Iron and Steel Institute, 174: 25-28.